# $H^{\pm} \to W^{\pm}\gamma$ and $H^{\pm} \to W^{\pm}Z$ in two-Higgs-doublet models: Large-fermion-mass limit

Michel Capdequi Peyranère
*Laboratoire de Physique Mathematique, Universite des Sciences et Techniques du Languedoc, Place Eugene Bataillon, 34095 Montpellier CEDEX 5, France*

Howard E. Haber and Paulo Irulegui
*Santa Cruz Institute for Particle Physics, University of California, Santa Cruz, California 95064*
(Received 9 January 1991)

In two-Higgs-doublet models, the $H^{\pm}W^{\mp}V$ vertex ($V=Z$ or $\gamma$) does not occur at the tree level, but is generated at one-loop order. We derive explicit formulas for the contribution of a weak doublet of fermions $(t,b)$ to the $H^{\pm} \to W^{\pm}Z$ amplitude in the limit of large fermion masses that appear in the internal loop. In this limit, the amplitude grows as the square of the fermion masses for $m_t \neq m_b$, and is constant if $m_t = m_b$. In contrast, the $H^{\pm} \to W^{\pm}\gamma$ amplitude approaches a constant (which depends on $m_t/m_b$) in the large-fermion-mass limit. Asymptotic results for the contribution of a heavy supersymmetric family are also given. The observability of $H^{\pm} \to W^{\pm}Z$ at a future supercollider requires either $m_{H^{\pm}} < m_t$ and a large $t$-quark mass, or the existence of a fourth-generation nondegenerate quark doublet.

## I. INTRODUCTION

The pursuit of the Higgs boson is one of the primary goals of the present and next generation of colliders [1]. Much effort has been devoted to devising strategies for discovering the neutral Higgs boson of the standard model. However, nearly all nonminimal extensions of the standard model contain charged Higgs bosons as well. Charged Higgs bosons with $m_{H^+} \lesssim \sqrt{s}/2$ can be produced and detected at an $e^+e^-$ collider with center-of-mass energy $\sqrt{s}$. Thus, when the CERN collider LEP II runs in the mid-1990's, charged Higgs bosons with $m_{H^+} \lesssim m_W$ will have been discovered or ruled out. To probe larger Higgs-boson masses, a supercollider will be required. In the absence of an $e^+e^-$ supercollider in the near future, we will have to depend on the Superconducting Super Collider (SSC) to probe heavier charged Higgs bosons. This is a daunting task; at present, it is not known how to detect charged Higgs bosons at a hadron supercollider if $m_{H^+} > m_t$ [2]. Although production cross sections are large, the dominant decay mode $H^+ \to t\bar{b}$ will be swamped by the QCD background. Thus the only hope may be to find some exotic decay mode with a more promising signature, but with a branching ratio large enough to provide a sufficient number of events for detection.

Here we shall focus on the rate decays $H^{\pm} \to W^{\pm}\gamma$ [3] and $H^{\pm} \to W^{\pm}Z$. In models with only Higgs doublets and singlets, these decay modes can only occur at the one-loop level [4]. The absence of a tree-level $H^{\pm}W^{\mp}\gamma$ vertex is a consequence of the conservation of the electromagnetic current. On the other hand, a tree-level $H^{\pm}W^{\mp}Z$ vertex can exist in models with more complicated Higgs multiplets (e.g., triplets). Thus detection of a charged-Higgs-boson decay into $WZ$ at a substantial rate would imply either that the one-loop decay amplitude in a multidoublet model was unexpectedly enhanced, or it would indicate the existence of a more exotic Higgs structure. In this paper we explore this first possibility by computing the decay rates for $H^{\pm} \to W^{\pm}\gamma$ and $H^{\pm} \to W^{\pm}Z$ in a two-Higgs-doublet extension of the standard model.

Our calculations indicate that the branching ratios for $H^{\pm} \to W^{\pm}\gamma$ and $H^{\pm} \to W^{\pm}Z$ may be large enough such that these decays could be detected at the SSC. As a figure of merit, imagine starting with $10^6$ charged Higgs bosons, which is the expected number [5] produced at the SSC per year for $m_{H^+} = 200$ GeV, with an integrated luminosity of $10^4$ pb$^{-1}$. If we demand that the final-state $W$ and $Z$ decay to charged leptons ($e$ or $\mu$), then we must require $B(H^{\pm} \to W^{\pm}\gamma) \gtrsim 5 \times 10^{-5}$ and $B(H^{\pm} \to W^{\pm}Z) \gtrsim 10^{-3}$ in order to produce ten signal events per year. We have found [6] that in the two-Higgs-doublet model, the branching ratio for $H^{\pm} \to W^{\pm}\gamma$ tends to be smaller than $10^{-4}$, whereas the branching ratio for $H^{\pm} \to W^{\pm}Z$ can be as large as $10^{-2}$. The potentially large branching ratio in the latter case can occur because the $H^{\pm} \to W^{\pm}Z$ decay amplitude is particularly sensitive to the existence of very heavy fermions. For example, in the case of the third generation of quarks $(t,b)$, we find that the amplitude for $H^{\pm} \to W^{\pm}Z$ grows like $m_t^2$, for $m_t \gg m_W$. This enhancement may be large enough to permit the detection of this decay mode at the SSC. At an $e^+e^-$ supercollider, discovery of a charged Higgs boson should be straightforward [7]. However, the total number of charged-Higgs-boson events will not be large. We note that [1] $\sigma(e^+e^- \to H^+H^-) \simeq 0.3R$ (where $R = 86.8$ fb for a 1-TeV linear collider). An integrated luminosity of 5000 $R^{-1}$ per year (see, e.g., Ref. [8]) would correspond to only 1500 Higgs-boson pairs. Clearly, $H^{\pm} \to W^{\pm}\gamma$ would not be observable. If the branching ratio for $H^{\pm} \to W^{\pm}Z$ were significantly enhanced, it might be detectable at an $e^+e^-$ supercollider, assuming that the $W^{\pm}Z$ pair could be observed (above background) in all of

its final-state decay modes with good efficiency.

In this paper we present simple analytical results for the quark and lepton loop contributions to $H^{\pm}\to W^{\pm}\gamma$ and $H^{\pm}\to W^{\pm}Z$ in a two-Higgs-doublet model, obtained in the limit of large quark and lepton masses. In Sec. II we discuss the expected behavior of the one-loop amplitudes in the limit of large fermion masses. In Sec. III we give the explicit asymptotic expressions for the amplitudes for $H^{\pm}\to W^{\pm}\gamma$ and $H^{\pm}\to W^{\pm}Z$ due to the contribution of a heavy-fermion doublet $(t,b)$. In Sec. IV we examine the minimal supersymmetric extension of the standard model (MSSM), which is a special case of the general two-Higgs-doublet model, and present the asymptotic contributions of a heavy-squark doublet to the $H^{\pm}$ decay amplitudes. In Sec. V, we discuss the implications of our results and make some concluding remarks. In Appendix A we present the exact results for the $H^{\pm}\to W^{\pm}\gamma$ and $H^{\pm}\to W^{\pm}Z$ amplitudes induced by quark and squark loops, as a function of the loop integrals. These integrals are defined in Appendix B, and simple analytic expressions which are valid in the limit of large internal loop mass are given.

A calculation which involves only the fermion loops and neglects the contributions of the gauge- and Higgs-boson loops is incomplete. In this paper we show that the fermion-loop contribution alone is an accurate approximation to the $H^{\pm}\to W^{\pm}Z$ amplitude only when there exists a heavy-mass-nondegenerate fermion doublet. On the other hand, it is only an order of magnitude estimate for the $H^{\pm}\to W^{\pm}\gamma$ amplitude. The full calculation, with all numerical results, will be given in a forthcoming paper [6]. In that paper we will present the computation of the gauge- and Higgs-boson loops and the contributions of the supersymmetric partners of the MSSM. A complete discussion of the phenomenological implications of our results will be given there. Recently, the evaluation of the one-loop-induced $H^{\pm}\to W^{\pm}Z$ vertex in the MSSM has been presented by Mendez and Pomarol [9]. Where our analyses overlap, our results are in qualitative agreement.

## II. CALCULATION OF $H^{\pm}\to W^{\pm}Z$ AND $H^{\pm}\to W^{\pm}\gamma$

We examine the decay of $H^{\pm}$ to $W^{\pm}Z$ and $W^{\pm}\gamma$ in a two-Higgs-doublet extension of the standard model. The fermion-loop graphs for these processes (in the unitary gauge) are shown in Fig. 1.

In our notation, $(t,b)$ represents a generic fermion (i.e., quark or lepton) doublet. Any one-loop graph with bubbles on the external legs of the gauge bosons gives no contribution; their amplitudes, by Lorentz invariance, must be proportional to $p\cdot\epsilon(p)=0$. The sum of all graphs involving fermion loops forms a gauge-invariant set. Thus we are free to use one gauge choice for this subset of graphs and a different choice for diagrams involving gauge- and Higgs-boson loops. Clearly, for fermion loops, the unitary gauge is the most convenient choice. In this gauge we find that all tadpole graphs sum to zero [10].

We begin by specifying our model. First, we have to choose the Higgs-boson–fermion coupling. In order to

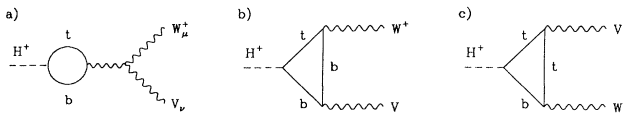


FIG. 1. Quark-loop graphs (excluding the tadpole graphs) for $H^{+}\to W^{+}V$, with $V=Z$ or $\gamma$.

guarantee the absence of Higgs-boson-mediated tree-level flavor-changing neutral currents, at most one Higgs doublet can couple to all quarks of a given electric charge [11]. We choose a Higgs-boson–fermion coupling in which the first doublet $(\Phi_1)$ couples only to down-type quarks and charged leptons, and the second doublet $(\Phi_2)$ couples only to up-type quarks and neutrinos. An important parameter of this model is

$$\tan\beta=\frac{v_2}{v_1}\ , \tag{1}$$

where $v_i\equiv\langle\Phi_i^0\rangle$ are the corresponding vacuum expectation values. The Higgs-boson–fermion coupling specified above is also the coupling pattern which appears in the minimal supersymmetric extension of the standard model. However, in the computation of the fermion-loop diagrams, we will not have to specify our model further.

The amplitudes for a charged scalar decaying into $WV$, where $V=Z$ or $\gamma$, can be written as

$$\mathcal{M}=\frac{g^3N_c\epsilon_V^{\nu *}\epsilon_W^{\mu *}}{16\pi^2 m_W\cos\theta_W}\mathcal{M}_{\mu\nu}\ , \tag{2}$$

where the number of colors, $N_c=3(1)$, for a quark (lepton) internal loop and

$$\mathcal{M}_{\mu\nu}=g_{\mu\nu}\mathcal{M}_1+p_{V_\mu}p_{W_\nu}\mathcal{M}_2+i\epsilon_{\mu\nu\rho\sigma}p_V^{\rho}p_W^{\sigma}\mathcal{M}_3\ . \tag{3}$$

Note that $\mathcal{M}_1$ has dimension of mass squared and receives contribution from all the diagrams of Fig. 1; $\mathcal{M}_2$ and $\mathcal{M}_3$ are dimensionless and originate from the triangle graphs [Figs. 1(b) and 1(c)]. In the large-fermion-mass limit, dimensionless quantities depend on fermion masses only through the ratio

$$R\equiv\frac{m_t^2}{m_b^2}\ . \tag{4}$$

All fermion-mass dependence comes from the $H^{+}tb$ coupling and the fermion propagators.

The behavior of $\mathcal{M}_{\mu\nu}$ in the large-fermion-mass limit is one of the primary goals of this paper. Simple dimensional arguments tell us what to expect. Consider first the case of $H^{\pm}\to W^{\pm}\gamma$. In this case gauge invariance requires

$$p_\gamma^{\mu}\mathcal{M}_{\mu\nu}=0\ , \tag{5}$$

which implies that

$$\mathcal{M}_1=-p_\gamma\cdot p_W\mathcal{M}_2=-\tfrac{1}{2}(m_{H^+}^2-m_W^2)\mathcal{M}_2\ . \tag{6}$$

That is, there are only two independent invariant amplitudes. In terms of an effective interaction, gauge invariance requires

$$\mathcal{L}_{\rm eff}=\frac{m_t}{m_W}H^+(g_2F_\gamma^{\mu\nu}F_{\mu\nu}^W+ig_3\epsilon_{\mu\nu\alpha\beta}F_\gamma^{\mu\nu}F_W^{\alpha\beta})\ , \tag{7}$$

where the factor $m_t/m_W$ originates from the $H^+tb$ vertex. The operators in Eq. (7) have dimension 5, which implies that as $m_b,m_t\to\infty$, $g_2$ and $g_3$ must be of the form $g(R)/m_t$, where $g(R)$ is a dimensionless function of the fermion masses. Hence it follows that $\mathcal{M}_{\mu\nu}$ must also be a dimensionless function of the fermion masses, which approaches a fixed $R$-dependent constant, in the large-fermion-mass limit.

Second, we consider the case of $H^{\pm}\to W^{\pm}Z$. In this case there is no corresponding gauge-invariance condition. Thus the three invariant amplitudes of Eq. (3) are independent. In terms of an effective interaction, in addition to replacing $F_\gamma^{\mu\nu}$ with $F_Z^{\mu\nu}$ in Eq. (7), we must also allow for

$$\mathcal{L}_{\rm eff}=\frac{m_t}{m_W}g_1H^+W^\mu Z_\mu\ . \tag{8}$$

This is a dimension-3 operator, which implies that $g_1$ must be of the form $m_tg(R)$, in the limit of large $m_b$ and $m_t$. Hence, in this case, $\mathcal{M}_1$ will grow *quadratically* with the fermion mass. The nonvanishing of the fermion-loop contributions in the large-fermion-mass limit is an example of the violation of decoupling which can occur in spontaneously broken gauge theories with axial-vector couplings [12]. In the next section, we provide the explicit limiting formulas which demonstrate the above remarks.

For completeness, we record here the formulas for the charged-Higgs-boson partial widths in terms of the invariant amplitudes defined above:

$$\Gamma(H^{\pm}\to W^{\pm}Z)=\frac{g^6N_c^2\lambda^{1/2}}{2^{16}\pi^5m_W^6m_H^3}[4(\lambda+12m_W^2m_Z^2)|\mathcal{M}_1|^2+\lambda^2|\mathcal{M}_2|^2+8\lambda m_W^2m_Z^2|\mathcal{M}_3|^2+4\lambda(m_H^2-m_W^2-m_Z^2)\mathrm{Re}\mathcal{M}_1\mathcal{M}_2^*]\ , \tag{9}$$

where $\lambda\equiv(m_H^2-m_W^2-m_Z^2)^2-4m_W^2m_Z^2$ and

$$\Gamma(H^{\pm}\to W^{\pm}\gamma)=\frac{g^6N_c^2m_H^3}{2^{13}\pi^5m_W^2\cos^2\theta_W}\left[1-\frac{m_W^2}{m_H^2}\right]^3\times(|\mathcal{M}_2|^2+|\mathcal{M}_3|^2)\ , \tag{10}$$

where we have used Eq. (6) to eliminate $\mathcal{M}_1$. One can easily check that by applying Eq. (6) to Eq. (9) and setting $m_Z=0$, we recover Eq. (10).

## III. LARGE-FERMION-MASS LIMIT

From the exact expressions for the amplitude coefficients $\mathcal{M}_1$, $\mathcal{M}_2$, and $\mathcal{M}_3$ given in Appendix A, we have derived the leading terms in the limit of large fermion masses in the loops by using the asymptotic formulas for the loop integrals given in Appendix B. We use the notation $(t,b)$ to denote a generic fermion weak doublet with corresponding electric charges $Q_t$ and $Q_b$. Thus the formulas presented below can be evaluated for both quark and lepton loops. Note that $Q_t-Q_b=1$, which is sometimes used in the derivation of the formulas given below. We present asymptotic formulas for $\mathcal{M}_1$, $\mathcal{M}_2$, and $\mathcal{M}_3$ in three cases: (i) a quark doublet with $m_t\gg m_b$, (ii) a quark doublet with $m_b\gg m_t$, and (iii) a doublet of nearly mass-degenerate quarks. Using the formulas of Appendixes A and B, it is straightforward to derive more general asymptotic results which are applicable for any value of $R\equiv m_t^2/m_b^2$. We will use such results in our numerical comparisons in Sec. V, although we will not display the more general formulas here [13]. To fully exhibit the symmetry between cases (i) and (ii), we also use the notation $T_{3t}=\frac{1}{2}$ and $T_{3b}=-\frac{1}{2}$ for the third component of the weak isospin. However, we will use $T_{3t}+T_{3b}=0$ in deriving our final expressions.

### A. Quarks with $m_t\gg m_b$

$H^{\pm}\to W^{\pm}\gamma$:

$$\begin{aligned}&\mathcal{M}_1=-\tfrac{1}{2}(m_{H^+}^2-m_W^2)\mathcal{M}_2\ ,\\ &\mathcal{M}_2=-\tfrac{1}{12}(2Q_t+Q_b)\sin2\theta_W\cot\beta\ ,\\ &\mathcal{M}_3=\tfrac{1}{4}(Q_t+Q_b)\sin2\theta_W\cot\beta\ .\end{aligned} \tag{11}$$

$H^{\pm}\to W^{\pm}Z$:

$$\begin{aligned}&\mathcal{M}_1=\tfrac{1}{2}m_t^2\cot\beta T_{3t}\ ,\\ &\mathcal{M}_2=\tfrac{1}{12}[T_{3t}+(2Q_t+Q_b)2\sin^2\theta_W]\cot\beta\ ,\\ &\mathcal{M}_3=-\tfrac{1}{4}[T_{3t}+(Q_t+Q_b)2\sin^2\theta_W]\cot\beta\ .\end{aligned} \tag{12}$$

### B. Quarks with $m_b\gg m_t$

$H^{\pm}\to W^{\pm}\gamma$:

$$\begin{aligned}&\mathcal{M}_1=-\tfrac{1}{2}(m_{H^+}^2-m_W^2)\mathcal{M}_2\ ,\\ &\mathcal{M}_2=-\tfrac{1}{12}(Q_t+2Q_b)\sin2\theta_W\tan\beta\ ,\\ &\mathcal{M}_3=-\tfrac{1}{4}(Q_t+Q_b)\sin2\theta_W\tan\beta\ .\end{aligned} \tag{13}$$

$H^{\pm}\to W^{\pm}Z$:

$$\begin{aligned}&\mathcal{M}_1=\tfrac{1}{2}m_b^2\tan\beta T_{3b}\ ,\\ &\mathcal{M}_2=\tfrac{1}{12}[T_{3b}+(Q_t+2Q_b)2\sin^2\theta_W]\tan\beta\ ,\\ &\mathcal{M}_3=-\tfrac{1}{4}[T_{3b}+(Q_t+Q_b)2\sin^2\theta_W]\tan\beta\ .\end{aligned} \tag{14}$$

It is easy to show that $\mathcal{M}_1$ and $\mathcal{M}_2$ are invariant and $\mathcal{M}_3$ changes sign under the interchange $t \leftrightarrow b$ and $\tan\beta \leftrightarrow \cot\beta$. The latter sign change is due to the behavior under the above interchange of the term proportional to $\gamma_5$ in the $H^+\bar{t}b$ coupling:

$$\frac{ig}{2\sqrt{2}m_W}[(m_b\tan\beta+m_t\cot\beta) +(m_b\tan\beta-m_t\cot\beta)\gamma_5] . \quad (15)$$

This provides us with an additional check of our calculation. For example, the two limiting cases just given are related by the above interchange. Thus we disagree with the conclusions of Ref. [14] that the $H^\pm \to W^\pm Z$ amplitude vanishes in the limit $m_b \to 0$.

### C. Nearly mass-degenerate quarks

$H^\pm \to W^\pm\gamma$:

$$\begin{aligned}\mathcal{M}_1 &= -\tfrac{1}{2}(m_{H^+}^2 - m_W^2)\mathcal{M}_2 ,\\ \mathcal{M}_2 &= -\tfrac{1}{24}\sin 2\theta_W[(Q_t+3Q_b)\tan\beta \\ &\qquad +(3Q_t+Q_b)\cot\beta] ,\\ \mathcal{M}_3 &= -\tfrac{1}{12}\sin 2\theta_W[(Q_t+2Q_b)\tan\beta \\ &\qquad -(2Q_t+Q_b)\cot\beta] .\end{aligned} \quad (16)$$

$H^\pm \to W^\pm Z$:

$$\begin{aligned}\mathcal{M}_1 &= \tfrac{1}{12}(m_t^2-m_b^2)(\tan\beta+\cot\beta)(T_{3t}-T_{3b}) \\ &\quad -\tfrac{1}{2}(m_{H^+}^2 - m_W^2 - m_Z^2)\mathcal{M}_2 \\ &\quad -\tfrac{1}{12}\sin^2\theta_W m_Z^2(\tan\beta+\cot\beta) ,\\ \mathcal{M}_2 &= \tfrac{1}{12}\sin^2\theta_W[(Q_t+3Q_b)\tan\beta+(3Q_t+Q_b)\cot\beta] ,\\ \mathcal{M}_3 &= \tfrac{1}{6}\sin^2\theta_W[(Q_t+2Q_b)\tan\beta-(2Q_t+Q_b)\cot\beta] .\end{aligned} \quad (17)$$

Note that the leading quadratic fermion-mass dependence in Eq. (17) vanishes in the limit $m_t \to m_b$, although terms which are constant in the large-fermion-mass limit remain. One check of our calculation is that the amplitudes above respect the symmetry $t \leftrightarrow b$, $\tan\beta \leftrightarrow \cot\beta$ (up to a sign change in $\mathcal{M}_3$), as previously noted. As an additional check, we observe that these amplitudes also satisfy the gauge-invariance condition given in Eq. (6) when $m_Z = 0$ and $m_t = m_b$. It is for this reason that the leading quadratic fermion-mass dependence in $\mathcal{M}_1(H^\pm \to W^\pm Z)$ must vanish when $m_t = m_b$.

## IV. LARGE-MASS SUPERSYMMETRIC LIMIT

The minimal supersymmetric model (MSSM) is perhaps the best motivated two-Higgs-doublet model [15, 16]. In this model the fermions $f$ are accompanied by scalar partners $\tilde{f}$. We therefore examine the effects of squark and slepton loop contributions to $H^\pm \to W^\pm\gamma$ and $H^\pm \to W^\pm Z$ shown in Fig. 2. In the unitary gauge, the tadpole graphs sum to zero, and so we omit them.

As before, we shall use the notation $(\tilde{t},\tilde{b})$ to denote a generic squark or slepton weak doublet. (For convenience, we will employ the term "squarks" to describe the members of this generic doublet.) Since squarks are scalars, there is no contribution to $\mathcal{M}_3$. The squark-loop contributions to the $H^\pm$ decay amplitudes are given in Appendix A. In this section we first examine the supersymmetric (SUSY) limit, where $M_{\tilde{q}_i} = m_{q_i}$. We follow the notation and conventions of the previous section. In the large-quark-mass (and therefore large-squark-mass) limit, the leading terms for the squark-loop contributions to $\mathcal{M}_1$ and $\mathcal{M}_2$ are easily obtained. Note that the quark masses enter via the $H^+\tilde{t}\tilde{b}$ couplings (which are given in Ref. [16]).

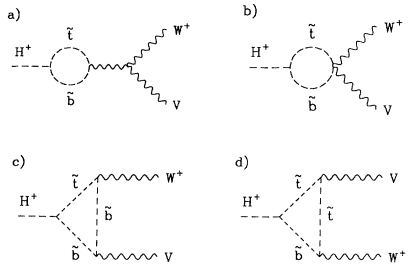


FIG. 2. Squark-loop graphs (excluding the tadpole graphs) for $H^+ \to W^+V$, with $V = Z$ or $\gamma$.

### A. Squarks with $m_t \gg m_b$ (SUSY limit)

$H^\pm \to W^\pm\gamma$:

$$\begin{aligned}\mathcal{M}_1 &= -\tfrac{1}{2}(m_{H^+}^2 - m_W^2)\mathcal{M}_2 ,\\ \mathcal{M}_2 &= -\tfrac{1}{12}\sin 2\theta_W(Q_t+2Q_b)\cot\beta .\end{aligned} \quad (18)$$

Note that $Q_t + 2Q_b = 0$ for $Q_t = \frac{2}{3}$ and $Q_b = -\frac{1}{3}$, and so the leading term cancels in this case and both amplitudes are of $O(1/m_t^2)$.

$H^\pm \to W^\pm Z$:

$$\begin{aligned}\mathcal{M}_1 &= \tfrac{1}{2}m_t^2\cot\beta\, T_{3t} ,\\ \mathcal{M}_2 &= \tfrac{1}{6}[T_{3t}+(Q_t+2Q_b)\sin^2\theta_W]\cot\beta .\end{aligned} \quad (19)$$

### B. Squarks with $m_b \gg m_t$ (SUSY limit)

$H^\pm \to W^\pm\gamma$:

$$\begin{aligned}\mathcal{M}_1 &= -\tfrac{1}{2}(m_{H^+}^2 - m_W^2)\mathcal{M}_2 ,\\ \mathcal{M}_2 &= -\tfrac{1}{12}\sin 2\theta_W(2Q_t+Q_b)\tan\beta .\end{aligned} \quad (20)$$

$H^\pm \to W^\pm Z$:

$$\begin{aligned}\mathcal{M}_1 &= \tfrac{1}{2}m_b^2\tan\beta\, T_{3b} ,\\ \mathcal{M}_2 &= \tfrac{1}{6}[T_{3b}+(2Q_t+Q_b)\sin^2\theta_W]\tan\beta .\end{aligned} \quad (21)$$

### C. Nearly mass-degenerate squarks (SUSY limit)

$$
\begin{aligned}
&H^{\pm}\to W^{\pm}\gamma:\\
&\mathcal{M}_1=-\tfrac{1}{2}(m_{H^+}^2-m_W^2)\mathcal{M}_2\ ,\\
&\mathcal{M}_2=-\tfrac{1}{24}(Q_t+Q_b)\sin 2\theta_W(\tan\beta+\cot\beta)\ .
\end{aligned}
\tag{22}
$$

$$
\begin{aligned}
&H^{\pm}\to W^{\pm}Z:\\
&\mathcal{M}_1=\tfrac{1}{12}(m_t^2-m_b^2)(\cot\beta+\tan\beta)(T_{3t}-T_{3b})\\
&\qquad-\tfrac{1}{2}(m_{H^+}^2-m_W^2-m_Z^2)\mathcal{M}_2\ ,\\
&\mathcal{M}_2=\tfrac{1}{12}(Q_t+Q_b)\sin^2\theta_W[\tan\beta+\cot\beta]\ .
\end{aligned}
\tag{23}
$$

The structure of these amplitudes are very similar to those found in Sec. III. As before, we note the invariance of the amplitudes under $t\leftrightarrow b$ and $\cot\beta\leftrightarrow\tan\beta$. Moreover, as in the quark case, the leading quadratic fermion-mass dependence of $\mathcal{M}_1(H^{\pm}\to W^{\pm}Z)$ vanishes in the limit $m_t\to m_b$. To obtain the contribution of one heavy supersymmetric family of fermions and their scalars partners, one simply adds these results to those obtained in Sec. III. Note in particular that as long as $m_t\neq m_b$, the quadratic behavior of $\mathcal{M}_1$ on $m_t$ and $m_b$ survives, even in the supersymmetric limit.

### D. Squarks with large SUSY breaking

We now briefly turn to the case where supersymmetry is broken. For simplicity, we shall ignore squark mixing and assume that $\tilde{q}_L$ and $\tilde{q}_R$ are the appropriate squark-mass eigenstates. Then, in our calculation, only $\tilde{q}_L$ appears, since $\tilde{q}_R$ does not couple to the $W^{\pm}$. Let us assume that the squarks acquire large soft-symmetry-breaking scalar masses, so that $M_{\tilde{q}}\gg m_q$. Using the squark-loop formulas given in Appendix A, we can easily derive the asymptotic formula appropriate for the large-squark-mass limit. In contrast with the results given above, the fermion masses (which appear squared in the $H^+\tilde{t}\,\tilde{b}$ coupling) are held fixed. As a result, amplitudes which were formerly constant in the large-squark-mass limit will now vanish quadratically with $M_{\tilde{q}}$. Only one amplitude survives in the large-squark-mass limit:

$$
\begin{aligned}
\mathcal{M}_1(H^{\pm}\to W^{\pm}Z)=&\frac{T_{3t}(m_b^2\tan\beta+m_t^2\cot\beta-m_W^2\sin 2\beta)}{2(M_{\tilde{t}}^2-M_{\tilde{b}}^2)}\\
&\times\left[M_{\tilde{t}}^2+M_{\tilde{b}}^2-\frac{2M_{\tilde{t}}^2M_{\tilde{b}}^2}{M_{\tilde{t}}^2-M_{\tilde{b}}^2}\ln\left[\frac{M_{\tilde{t}}^2}{M_{\tilde{b}}^2}\right]\right]\ .
\end{aligned}
\tag{24}
$$

Note that in the limit of $M_{\tilde{t}}=M_{\tilde{b}}$, this amplitude also vanishes, in which case the leading term which survives is of $O(1/M_{\tilde{q}}^2)$. Equation (24) indicates that infinitely massive (mass-nondegenerate) squark loops would contribute a constant amount to $\mathcal{M}_1(H^{\pm}\to W^{\pm}Z)$, whereas they decouple from all other one-loop-mediated Higgs-boson decays. However, this violation of decoupling is illusory. The soft-supersymmetry-breaking masses of $\tilde{t}_L$ and $\tilde{b}_L$ must be equal [since these are SU(2)×U(1)-conserving masses], so that the mass splitting between $\tilde{t}_L$ and $\tilde{b}_L$ can only come from electroweak effects. Thus it follows that the squark-loop contributions decouple in the limit of $M_{\tilde{q}}\gg m_q, m_Z$.

## V. RESULTS AND CONCLUSIONS

We have presented simple analytic formulas for the invariant amplitudes of $H^{\pm}\to W^{\pm}\gamma$ and $H^{\pm}\to W^{\pm}Z$ in the large-fermion-mass limit in the two-Higgs-doublet model. The accuracy of these formulas are illustrated in Figs. 3 and 4. In both figures we assume $m_{H^+}=200$ GeV and $\tan\beta=2$.

In Fig. 3 we plot the contributions of a generic quark doublet $(t,b)$ to $\mathcal{M}_1$, the coefficient of the $g_{\mu\nu}$ term in the amplitude in Eq. (3), as a function of $m_t$. Four cases are shown: $H^{\pm}\to W^{\pm}Z$ for $m_b=100$ GeV (exact and asymptotic results), $H^{\pm}\to W^{\pm}Z$ for $m_b=m_t$ (exact), and $H^{\pm}\to W^{\pm}\gamma$ for $m_b=100$ GeV (exact). The asymptotic results for $H^{\pm}\to W^{\pm}Z$ were computed by making use of the results of Appendix B and are valid to leading order in $m_t^2$ and/or $m_b^2$ for arbitrary $m_t^2/m_b^2$. Special cases of these formulas were presented in Sec. III. Comparing the asymptotic result ($A$) to the exact one-loop result ($E$), we find that $|E-A|/E$ is 30% for $m_t=200$ GeV and decreases quadratically to 1% for $m_t=10^3$ GeV. The plot for $H^{\pm}\to W^{\pm}Z$, with $m_b=m_t$, shows that in this case $\mathcal{M}_1$ is asymptotically independent of $m_t$, as indicated by the limiting formulas of Sec. III. Similarly, the curve for $H^{\pm}\to W^{\pm}\gamma$ also shows no asymptotic dependence on $m_t$, as expected. The use of $m_b=100$ GeV in this figure is

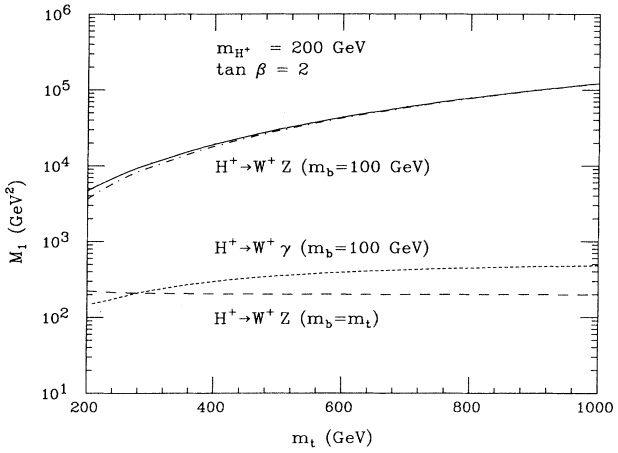


FIG. 3. Contribution of a $(t,b)$ quark loop to the amplitude $\mathcal{M}_1$ as a function of $m_{t'}$, a generic top-quark mass. The solid line is a plot of $\mathcal{M}_1(H^{\pm}\to W^{\pm}Z)$, computed exactly at one loop, with $m_b=100$ GeV, and the dotted line is the corresponding asymptotic result (valid in the large-fermion-mass limit). The dashed line is the exact result for $H^{\pm}\to W^{\pm}Z$ with $m_b=m_t$, and the short-dashed line is the exact one-loop result for $H^{\pm}\to W^{\pm}\gamma$ with $m_b=100$ GeV.

merely illustrative, in order to exhibit the asymptotic behavior of $\mathcal{M}_1$ for the case of nondegenerate quarks. In particular, $m_t - m_b \gtrsim 200$ GeV is not consistent with the experimental constraints on the $\rho$ parameter (we assume $|\rho - 1| \lesssim 0.01$ [17]).

In Fig. 4 we examine the effect of a fourth generation of quarks $(t', b')$. We plot the branching ratios of $H^+ \to t\bar{b}$, $H^+ \to W^+Z$ (exact and asymptotic), and $H^+ \to W^+\gamma$ (exact), as a function of $m_{t'}$. For the third family top quark, we assume $m_t = 100$ GeV, and for the fourth family, we take $m_{t'} - m_{b'} = 160$ GeV, in order that $|\rho - 1| \lesssim 0.01$. In this case, $m_{H^+} > m_t + m_b$, and $H^+ \to t\bar{b}$ is the dominant decay mode. The branching ratios to $W^+Z$ and $W^+\gamma$ were computed by evaluating the fermion-loop contributions only. This is an excellent approximation in the $W^+Z$ case because of the quadratic sensitivity to the fourth-generation quark mass. For $W^+\gamma$ the result is less reliable; the effects of the gauge- and Higgs-boson loops are at least as important as the fermion loops. We find [6] that a typical result is $B(H^+ \to W^+\gamma) \sim 10^{-5}$. The branching ratio required for $H^+ \to W^+Z$ detection at the SSC, $\gtrsim 10^{-3}$, can be obtained for $m_{t'} \gtrsim 500$ GeV. (Note that the branching ratio decreases as $m_{t'} - m_{b'}$ is taken smaller.) If $m_t + m_b > m_{H^+}$, $H^+ \to t\bar{b}$ is forbidden, and the contribution of the third family alone in $H^+ \to W^+Z$ is enough to make this one of the dominant $H^+$ decay modes. (The other major decay mode would be $H^+ \to W^+h^0$, where $h^0$ is the lightest neutral $CP$-even Higgs scalar.) We find $B(H^+ \to W^+Z) = 6 \times 10^{-3}$ for $m_t \geq m_{H^+} = 200$ GeV and $\tan\beta = 2$; even larger values of the branching ratio are possible as $\tan\beta$ approaches unity. Further phenomenological implications will be discussed in a forthcoming publication [6], where we will examine the effects of gauge- and Higgs-boson loops and the effects of including the supersymmetric partners of the MSSM. We already noted at the end of Sec. IV that the effects of very massive squarks and sleptons decouple. The same is true for very heavy neutralinos and charginos (the fermionic partners of the gauge and Higgs bosons). For moderately sized supersymmetric masses, all these effects are roughly of the same order of magnitude, and a complete computation is required.

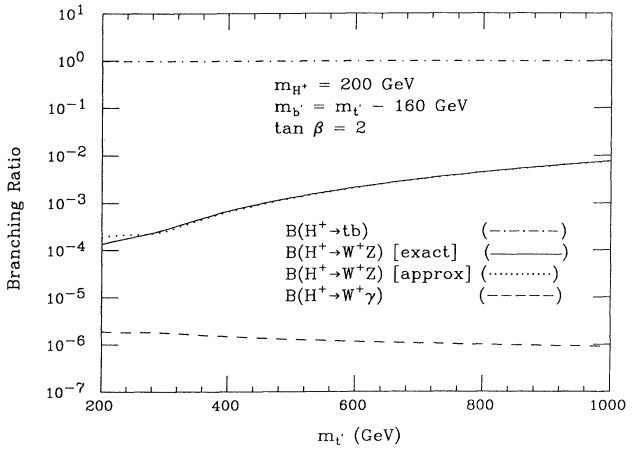


FIG. 4. Contribution of a fourth-generation quark doublet $(t', b')$ to the branching ratios for $H^\pm \to W^\pm Z$ and $H^\pm \to W^\pm\gamma$. We assume that $m_t = 100$ GeV and $m_{t'} - m_{b'} = 160$ GeV. The decay $H^+ \to t\bar{b}$ occurs with nearly 100% branching ratio (dot-dashed line). Also shown are the exact (solid line) and asymptotic (dotted line) one-loop results for $H^\pm \to W^\pm Z$ and the exact one-loop result for $H^\pm \to W^\pm\gamma$ (dashed line).

In summary, the $H^\pm \to W^\pm Z$ sensitivity to very heavy fermions can impose nontrivial constraints on Higgs models and the possible existence of new generations of quarks (and leptons). If $m_{H^+} \gtrsim m_t$, $H^+ \to t\bar{b}$ is the dominant decay mode, and detection of $H^\pm \to W^\pm Z$ at the SSC would indicate either an exotic Higgs structure consisting of triplets or higher-dimensional multiplets or the existence of a new heavy generation of fermions in the case of a multi-Higgs-doublet model (with or without supersymmetry). If $m_{H^+} \lesssim m_t + m_b$, $H^\pm \to W^\pm Z$ can be one of the dominant decay modes of $H^+$ and may be detectable at the SSC. At a future $e^+e^-$ supercollider, the limits on machine luminosity impose severe restrictions on the observability of rare decays of the charged Higgs boson. However, backgrounds are less severe (compared to the SSC), and it might be possible to detect $H^\pm \to W^\pm Z$ if its branching ratio is significantly enhanced. Clearly, the discovery of the one-loop decays studied in this paper would put strong constraints on our understanding of the physics beyond the standard model.

## ACKNOWLEDGMENTS

M.C.P. would like to thank the Santa Cruz Institute for Particle Physics and the UCSC Physics Department for their kind hospitality and warm atmosphere during his sabbatical. He acknowledges support of Unité de Recherche Associée au CNRS URA 768. H.E.H. would like to thank Fernand Renard and the Laboratoire de Physqiue Mathematique of USTL in Montpellier for their support and hospitality during his visits, where some of this work was done. This work was also supported in part by the U.S. Department of Energy. The work of P.I. was supported, in part, by the CAPES-Coordenação de Aperfeiçoamento de Pessoal de Nível Superior (Brazil) and the U.S. Department of Energy.

## APPENDIX A: EXACT QUARK AND SQUARK ONE-LOOP AMPLITUDES

In this Appendix we present the exact expressions for the invariant amplitudes $\mathcal{M}_1$, $\mathcal{M}_2$, and $\mathcal{M}_3$, defined in Eq. (3), as a function of the loop integrals defined in Appendix B. We use the notation $(t, b)$ to denote a generic fermion weak doublet, with corresponding electric charges $Q_t$ and $Q_b$ (in units of $e > 0$) and third component of weak isospin $T_{3t} = -T_{3b} = \frac{1}{2}$. Note that, in general, $Q_t - Q_b = 1$. The $Zf\bar{f}$ tree-level coupling is defined by $ig\gamma_\mu(G_f^L P_L + G_f^R P_R)/\cos\theta_W$, where $P_{R,L} = \frac{1}{2}(1 \pm \gamma_5)$ and

$$G_f^L = -T_{3f} + Q_f \sin^2\theta_W ,$$

$$G_f^R = Q_f \sin^2\theta_W .$$

From the kinematics with $p_H=p_W+p_Z$,

$$P_H\cdot p_W=\tfrac{1}{2}(m_{H^+}^2+m_W^2-m_Z^2)\ ,$$
$$P_H\cdot p_Z=\tfrac{1}{2}(m_{H^+}^2-m_W^2+m_Z^2)\ ,$$
$$P_Z\cdot p_W=\tfrac{1}{2}(m_{H^+}^2-m_W^2-m_Z^2)\ .$$

In each formula presented below, all the $B_i$ functions in the same formula have the same arguments; arguments of $C$ and $\tilde{C}$ are defined as

$$C_{0;ij}=C_{0;ij}(p_W^2,p_Z^2,p_H^2;m_t^2,m_b^2,m_b^2)\ ,$$
$$C_{0;ij}=C_{0;ij}(p_W^2,p_Z^2,p_H^2;m_t^2,m_b^2,m_b^2)\ .$$

In $H^{\pm}\to W^{\pm}\gamma$, replace $p_Z$ with $p_\gamma$ and $m_Z$ with $m_\gamma=0$. Each graph will be referenced via a superscript in $\mathcal{M}$ with the letter that labels its figure. Our results for $H^{\pm}\to W^{\pm}\gamma$ are in slight disagreement with those in Ref. [3] (see Ref. [18]). In regard to the quark- and squark-loop contributions, we only differ on the sign of $\mathcal{M}_3^b$ presented below.

### 1. $H^{\pm}\to W^{\pm}\gamma$

*Quark loops* (factoring out a common factor of $+\frac{1}{2}\sin 2\theta_W$):

$$\mathcal{M}_1^a=-m_t^2\cot\beta[B_0(m_{H^+}^2;m_t^2,m_b^2)+B_1]-m_b^2\tan\beta(B_1)\ ,$$
$$\mathcal{M}_1^b=-Q_b m_t^2\cot\beta[(p_H\cdot p_W-m_b^2)C_0+(p_H+p_W)\cdot p_W C_{11}+(p_H+p_W)\cdot p_\gamma C_{12}+m_W^2 C_{21}$$
$$+2p_W\cdot p_\gamma C_{23}+2C_{24}-\tfrac{1}{2}]+Q_b m_b^2\tan\beta(p_W\cdot p_\gamma C_{11}+2C_{24})\ ,$$
$$\mathcal{M}_2^b=Q_b m_t^2\cot\beta(C_0+C_{11}+2C_{12}+2C_{23})+Q_b m_b^2\tan\beta(-C_{11}+2C_{12}+2C_{23})\ ,$$
$$\mathcal{M}_3^b=-Q_b m_t^2\cot\beta(C_0+C_{11})-Q_b m_b^2\tan\beta(C_{11})\ ,$$
$$\mathcal{M}_1^c=-Q_t m_t^2\cot\beta(p_H\cdot p_\gamma\tilde{C}_0+p_W\cdot p_\gamma\tilde{C}_{12}-2\tilde{C}_{24})$$
$$-Q_t m_b^2\tan\beta(-m_t^2\tilde{C}_0+p_W\cdot p_\gamma\tilde{C}_{12}+m_W^2\tilde{C}_{22}+2p_W\cdot p_\gamma\tilde{C}_{23}+2\tilde{C}_{24}-\tfrac{1}{2})\ ,$$
$$\mathcal{M}_2^c=Q_t m_t^2\cot\beta(\tilde{C}_0+3\tilde{C}_{12}+2\tilde{C}_{23})+Q_t m_b^2\tan\beta(\tilde{C}_{12}+2\tilde{C}_{23})\ ,$$
$$\mathcal{M}_3^c=-Q_t m_t^2\cot\beta(\tilde{C}_0+\tilde{C}_{12})-Q_t m_b^2\tan\beta(\tilde{C}_{12})\ .$$

*Squark loops* [factoring out a common factor of $\frac{1}{2}\sin 2\theta_W(m_b^2\tan\beta+m_t^2\cot\beta-m_W^2\sin 2\beta)$]:

$$\mathcal{M}_1^a=\tfrac{1}{2}B_0(m_{H^+}^2;m_t^2,m_b^2)+B_1,\quad \mathcal{M}_1^b=\tfrac{1}{2}(Q_t+Q_b)B_0(m_{H^+}^2;m_t^2,m_b^2),\quad \mathcal{M}_1^c=-2Q_b(C_{24})\ ,$$
$$\mathcal{M}_2^c=-2Q_b(C_{12}+C_{23}),\quad \mathcal{M}_1^d=-2Q_t(\tilde{C}_{24}),\quad \mathcal{M}_2^d=-2Q_t(\tilde{C}_{12}+\tilde{C}_{23})\ .$$

### 2. $H^{\pm}\to W^{\pm}Z$

To simplify the expressions for $\mathcal{M}_1^b$ and $\mathcal{M}_1^c$, one can make use of the exact relations

$$m_W^2 C_{21}+m_Z^2 C_{22}+2p_W\cdot p_Z C_{23}+4C_{24}-\tfrac{1}{2}=B_0(m_Z^2,m_b^2,m_b^2)+m_t^2 C_0\ ,$$
$$m_Z^2\tilde{C}_{21}+m_W^2\tilde{C}_{22}+2p_W\cdot p_Z\tilde{C}_{23}+4\tilde{C}_{24}-\tfrac{1}{2}=B_0(m_W^2,m_t^2.m_b^2)+m_t^2\tilde{C}_0\ .$$

We make use of these relations in our numerical analysis. However, in order to calculate the large-fermion-mass limit using the formulas for the loop integrals given in Appendix B, it is more convenient *not* to make the above substitutions. We then find the following:

*Quark loops:*

$$\mathcal{M}_1^a=\sin^2\theta_W\{m_t^2\cot\beta[B_0(m_{H^+}^2;m_t^2,m_b^2)+B_1]+m_b^2\tan\beta B_1\}\ ,$$
$$\mathcal{M}_1^b=m_t^2\cot\beta G_b^L[p_H\cdot p_W C_0+(p_H+p_W)\cdot p_W C_{11}+(p_H+p_W)\cdot p_Z C_{12}+m_W^2 C_{21}+m_Z^2 C_{22}+2p_W\cdot p_Z C_{23}+2C_{24}-\tfrac{1}{2}]$$
$$-m_t^2\cot\beta G_b^R(m_b^2 C_0)+m_b^2\tan\beta G_b^L(m_W^2 C_{11}+p_W\cdot p_Z C_{12}+m_W^2 C_{21}+m_Z^2 C_{22}+2p_W\cdot p_Z C_{23}+2C_{24}-\tfrac{1}{2})$$
$$-m_b^2\tan\beta G_b^R(p_H\cdot p_W C_{11}+p_H\cdot p_Z C_{12}+m_W^2 C_{21}+m_Z^2 C_{22}+2p_W\cdot p_Z C_{23}+4C_{24}-\tfrac{1}{2})\ ,$$
$$\mathcal{M}_2^b=-m_t^2\cot\beta G_b^L(C_0+C_{11}+2C_{12}+2C_{23})-m_b^2\tan\beta G_b^L(C_{12}+2C_{23})+m_b^2\tan\beta G_b^R(C_{11}-C_{12})\ ,$$
$$\mathcal{M}_3^b=m_t^2\cot\beta G_b^L(C_0+C_{11})+m_b^2\tan\beta G_b^L(C_{12})+m_b^2\tan\beta G_b^R(C_{11}-C_{12})\ ,$$

$$\mathcal{M}_1^c = m_t^2\cot\beta G_t^L[p_H\cdot p_Z\tilde{C}_0+(p_H+p_Z)\cdot p_Z\tilde{C}_{11}+(p_H+p_Z)\cdot p_W\tilde{C}_{12}+m_Z^2\tilde{C}_{21}+m_W^2\tilde{C}_{22}+2p_W\cdot p_Z\tilde{C}_{23}+2\tilde{C}_{24}-\tfrac{1}{2}]$$
$$-m_t^2\cot\beta G_t^R(p_H\cdot p_Z\tilde{C}_{11}+p_H\cdot p_W\tilde{C}_{12}+m_Z^2\tilde{C}_{21}+m_W^2\tilde{C}_{22}+2p_W\cdot p_Z\tilde{C}_{23}+4\tilde{C}_{24}-\tfrac{1}{2})$$
$$+m_b^2\tan\beta G_t^L(m_Z^2\tilde{C}_{11}+p_W\cdot p_Z\tilde{C}_{12}+m_Z^2\tilde{C}_{21}+m_W^2\tilde{C}_{22}+2p_W\cdot p_Z\tilde{C}_{23}+2\tilde{C}_{24}-\tfrac{1}{2})-m_b^2\tan\beta G_t^R(m_t^2\tilde{C}_0)\ ,$$

$$\mathcal{M}_2^c = -m_t^2\cot\beta G_t^L(\tilde{C}_0+\tilde{C}_{11}+2\tilde{C}_{12}+2\tilde{C}_{23})+m_t^2\cot\beta G_t^R(\tilde{C}_{11}-\tilde{C}_{12})-m_b^2\tan\beta G_t^L(\tilde{C}_{12}+2\tilde{C}_{23})\ ,$$

$$\mathcal{M}_3^c = m_t^2\cot\beta G_t^L(\tilde{C}_0+\tilde{C}_{11})-m_t^2\cot\beta G_t^R(\tilde{C}_{11}-\tilde{C}_{12})+m_b^2\tan\beta G_t^L(\tilde{C}_{12})\ .$$

*Squark loops* [factoring out a common factor of $(m_b^2\tan\beta+m_t^2\cot\beta-m_W^2\sin 2\beta)$]:

$$\mathcal{M}_1^q = -\sin^2\theta_W[\tfrac{1}{2}B_0(m_{H^+}^2;m_{\tilde{t}}^2,m_{\tilde{b}}^2)+B_1]),\quad \mathcal{M}_1^b = -\tfrac{1}{2}\sin^2\theta_W(Q_t+Q_b)B_0(m_{H^+}^2;m_{\tilde{t}}^2,m_{\tilde{b}}^2),$$

$$\mathcal{M}_1^c = 2G_b^L(C_{24}),\quad \mathcal{M}_2^c = 2G_b^L(C_{12}+C_{23}),\quad \mathcal{M}_1^d = 2G_t^L(\tilde{C}_{24}),\quad \mathcal{M}_2^d = 2G_t^L(\tilde{C}_{12}+\tilde{C}_{23})\ .$$

## APPENDIX B: ONE-LOOP INTEGRALS

We use the standard notation for one-loop integrals [19]. However, in contrast to Ref. 19, we employ the metric and $\gamma$ matrix conventions of Bjorken and Drell [20]. We define

$$A_0(m^2) = -16\pi^2 i\int\frac{d^nq}{(2\pi)^n}\frac{1}{D_A}\ ,$$

$$B_0;B^\mu(p^2;m_a^2,m_b^2) = -16\pi^2 i\int\frac{d^nq}{(2\pi)^n}\frac{1;q^\mu}{D_B}\ ,$$

$$C_0;C^\mu;C^{\mu\nu}(p_1^2,p_2^2,p^2;m_a^2,m_b^2,m_c^2) = -16\pi^2 i\int\frac{d^nq}{(2\pi)^n}\frac{1;q^\mu;q^\mu q^\nu}{D_C}\ ,$$

where

$$D_A = (q^2-m^2)\ ,$$

$$D_B = (q^2-m_a^2)[(q+p)^2-m_b^2]\ ,$$

$$D_C = (q^2-m_a^2)[(q+p_1)^2-m_b^2][(q+p_1+p_2)^2-m_c^2]\ ,$$

for $p=-(p_1+p_2)$, with all momenta flowing into the graphs. By Lorentz invariance, $B^\mu$, $C^\mu$, and $C^{\mu\nu}$ can be decomposed as follows:

$$B^\mu = B_1 p^\mu\ ,$$

$$C^\mu = C_{11}p_1^\mu + C_{12}p_2^\mu\ ,$$

$$C^{\mu\nu} = C_{21}p_1^\mu p_1^\nu + C_{22}p_2^\mu p_2^\nu + C_{23}(p_1^\mu p_2^\nu + p_2^\mu p_1^\nu) + C_{24}g^{\mu\nu}\ .$$

In order to simplify notation for the $B$'s and $C$'s given in the Appendixes, we define

$$B_i = B_i(p_H^2;m_t^2,m_b^2)\ ,$$

$$\tilde{B}_1 = B_1(p_H^2;m_b^2,m_t^2)\ ,$$

$$C_{0;ij} = C_{0;ij}(p_W^2,p_Z^2,p_H^2;m_t^2,m_b^2,m_b^2)\ ,$$

$$\tilde{C}_{0;ij} = C_{0;ij}(p_Z^2,p_W^2,p_H^2;m_t^2,m_t^2,m_b^2)\ ,$$

with the $H^+$, $W$, and $Z$ momenta taken on shell. $B_0$ is symmetric under the interchange of $m_t$ and $m_b$. The symmetries of the $C_0$ under permutation of its arguments and other useful relations are given in Ref. [21]. Note that

$$\tilde{B}_1 = -B_0-B_1\ .$$

Furthermore, the $\tilde{C}_{ij}$ can be expressed as linear combinations of the $C_{ij}$. See Ref. [13] for these and additional relations among the loop functions.

In the large-fermion-mass limit, at least one of the internal fermion masses is much larger than $m_{H^+}$, $m_W$, and $m_Z$, and the $B$'s and $C$'s reduce to rather simple expressions. $\Delta$ is the divergent term $\Delta\equiv 2/(4-n)-\gamma_E+\ln 4\pi$, where $\gamma_E$ is the Euler constant and $n$ is the number of space-time dimensions; $\mu$ is the mass parameter introduced by dimensional regularization.

### 1. $(m_t/m_b)^2\equiv R\neq 0,\infty$

The results given below are valid for arbitrary $R$ as long as $m_t, m_b \gg m_W, m_Z, m_H$. Thus the cases of $R=0$ ($m_t=0$) and $R=\infty$ ($m_b=0$) must be treated separately. Nevertheless, one can check that those expressions below which have finite limits at $R=0$ or $\infty$ do indeed give the correct answers in these limits. The limit $R=1$ may appear singular, but all expressions below are in fact well behaved in this limit. However, for convenience, we shall list separately the behavior of the loop integrals near $R=1$:

$$A_0 = [\Delta-\ln(m^2/\mu^2)+1]m^2\ ,$$

$$B_0 = \Delta-\ln(m_b^2/\mu^2)+1-\frac{R\ln R}{R-1}+\frac{m_{H^+}^2}{2m_b^2}\left[\frac{1}{R-1}+\frac{2}{(R-1)^2}-\frac{2R\ln R}{(R-1)^3}\right]\ ,$$

$$B_1 = -\frac{1}{2}\left[\Delta-\ln(m_b^2/\mu^2)+\tfrac{3}{2}+\frac{1}{R-1}-\frac{R^2\ln R}{(R-1)^2}\right]\frac{-m_{H^+}^2}{6m_b^2}\left[\frac{2}{R-1}+\frac{9}{(R-1)^2}+\frac{6}{(R-1)^3}-\frac{6R^2\ln R}{(R-1)^4}\right]\ ,$$

$$C_0=\frac{1}{m_b^2}\left[\frac{1}{R-1}-\frac{R\ln R}{(R-1)^2}\right],\quad C_{11}=\frac{1}{m_b^2}\left[-\frac{\frac{3}{2}}{R-1}-\frac{1}{(R-1)^2}+\frac{R^2\ln R}{(R-1)^3}\right],$$

$$C_{12}=\tfrac{1}{2}C_{11},\quad C_{21}=\frac{1}{m_b^2}\left[\frac{\frac{11}{6}}{R-1}+\frac{\frac{5}{2}}{(R-1)^2}+\frac{1}{(R-1)^3}-\frac{R^3\ln R}{(R-1)^4}\right],$$

$$C_{22}=\tfrac{1}{3}C_{21},\quad C_{23}=\tfrac{1}{2}C_{21},$$

$$C_{24}=\frac{1}{4}\left[\Delta-\ln(m_b^2/\mu^2)+\frac{3}{2}+\frac{1}{R-1}-\frac{R^2\ln R}{(R-1)^2}\right]$$
$$+\frac{m_{H^+}^2+m_W^2}{24m_b^2}\left[\frac{2}{R-1}+\frac{9}{(R-1)^2}+\frac{6}{(R-1)^3}-\frac{6R^2\ln R}{(R-1)^4}\right]$$
$$-\frac{m_Z^2}{72m_b^2}\left[\frac{11}{R-1}+\frac{15}{(R-1)^2}+\frac{6}{(R-1)^3}-\frac{6R^3\ln R}{(R-1)^4}\right],$$

$$\tilde{B}_1=-\frac{1}{2}\left[\Delta-\ln(m_b^2/\mu^2)+\tfrac{1}{2}-\frac{1}{R-1}-\frac{R(R-2)\ln R}{(R-1)^2}\right]-\frac{m_{H^+}^2}{6m_b^2}\left[\frac{1}{R-1}-\frac{3}{(R-1)^2}-\frac{6}{(R-1)^3}+\frac{6R\ln R}{(R-1)^4}\right],$$

$$\tilde{C}_0=\frac{1}{m_b^2}\left[-\frac{1}{R-1}+\frac{\ln R}{(R-1)^2}\right],\quad \tilde{C}_{11}=\frac{1}{2m_b^2}\left[\frac{\frac{3}{2}}{R-1}+\frac{1}{(R-1)^2}-\frac{(2R-1)\ln R}{(R-1)^3}\right],$$

$$\tilde{C}_{12}=\frac{1}{m_b^2}\left[\frac{\frac{1}{2}}{R-1}+\frac{1}{(R-1)^2}-\frac{R\ln R}{(R-1)^3}\right],$$

$$\tilde{C}_{21}=\frac{1}{3m_b^2}\left[-\frac{\frac{11}{6}}{R-1}-\frac{\frac{5}{2}}{(R-1)^2}-\frac{1}{(R-1)^3}+\frac{3R\ln R}{(R-1)^3}+\frac{\ln R}{(R-1)^4}\right],$$

$$\tilde{C}_{22}=\frac{1}{m_b^2}\left[-\frac{\frac{1}{3}}{R-1}-\frac{\frac{3}{2}}{(R-1)^2}-\frac{1}{(R-1)^3}+\frac{R^2\ln R}{(R-1)^4}\right],$$

$$\tilde{C}_{23}=\frac{1}{m_b^2}\left[-\frac{\frac{5}{12}}{R-1}-\frac{\frac{5}{4}}{(R-1)^2}-\frac{\frac{1}{2}}{(R-1)^3}+\frac{R(R-\frac{1}{2})\ln R}{(R-1)^4}\right],$$

$$\tilde{C}_{24}=\frac{1}{4}\left[\Delta-\ln(m_b^2/\mu^2)+\frac{1}{2}-\frac{1}{R-1}-\frac{R(R-2)\ln R}{(R-1)^2}\right]$$
$$+\frac{(m_{H^+}^2+m_W^2)}{24m_b^2}\left[\frac{1}{R-1}-\frac{3}{(R-1)^2}-\frac{6}{(R-1)^3}+\frac{6R\ln R}{(R-1)^4}\right]$$
$$+\frac{m_Z^2}{72m_b^2}\left[\frac{2}{R-1}-\frac{3}{(R-1)^2}+\frac{6}{(R-1)^3}-\frac{6\ln R}{(R-1)^4}\right].$$

### 2. $m_t\simeq m_b$ ($R\simeq 1$)

$$B_0=\Delta-\ln(m_b^2/\mu^2)+\frac{m_{H^+}^2}{6m_b^2}-\tfrac{1}{2}(R-1),$$

$$B_1=-\frac{1}{2}\left[\Delta-\ln(m_b^2/\mu^2)+\frac{m_{H^+}^2}{6m_b^2}\right]+\tfrac{1}{6}(R-1),$$

$$C_0=-\frac{1}{2m_b^2}+\frac{R-1}{6m_b^2},\quad C_{11}=\frac{1}{3m_b^2}-\frac{R-1}{12m_b^2},$$

$$C_{12}=\frac{1}{6m_b^2}-\frac{R-1}{24m_b^2},\quad C_{21}=-\frac{1}{4m_b^2}+\frac{R-1}{20m_b^2},$$

$$C_{22}=-\frac{1}{12m_b^2}+\frac{R-1}{60m_b^2},\quad C_{23}=-\frac{1}{8m_b^2}+\frac{R-1}{40m_b^2},$$

$$C_{24}=\frac{1}{4}\left[\Delta-\ln(m_b^2/\mu^2)+\frac{m_{H^+}^2+m_W^2+m_Z^2}{12m_b^2}\right]$$
$$-\tfrac{1}{12}(R-1),$$

$$\tilde{B}=-\frac{1}{2}\left[\Delta-\ln(m_b^2/\mu^2)+\frac{m_{H^+}^2}{6m_b^2}\right]+\tfrac{1}{3}(R-1),$$

$$\tilde{C}_0=-\frac{1}{2m_b^2}-\frac{R-1}{6m_b^2},\quad \tilde{C}_{11}=\frac{1}{3m_b^2}-\frac{5(R-1)}{24m_b^2},$$

$$\tilde{C}_{12}=\frac{1}{6m_b^2}-\frac{R-1}{12m_b^2},\quad \tilde{C}_{21}=-\frac{1}{4m_b^2}+\frac{3(R-1)}{20m_b^2},$$

$$\tilde{C}_{22}=-\frac{1}{12m_b^2}+\frac{R-1}{30m_b^2},\quad \tilde{C}_{23}=-\frac{1}{8m_b^2}+\frac{7(R-1)}{120m_b^2},$$

$$\tilde{C}_{24}=\frac{1}{4}\left[\Delta-\ln(m_b^2/\mu^2)+\frac{m_{H^+}^2+m_W^2+m_Z^2}{12m_b^2}\right]$$

$$-\tfrac{1}{6}(R-1).$$

### 3. $m_t=0$ ($R=0$)

One cannot simply take the $R\to 0$ limit of the formulas of Appendix B 1 since some of the results would diverge. A separate calculation shows that these divergences are cut off by $m_Z$. The results below are valid for $m_t \ll m_Z, m_W, m_H \ll m_b$:

$$B=\Delta-\ln(m_b^2/\mu^2)+1+\frac{m_{H^+}^2}{2m_b^2},$$

$$B_1=-\tfrac{1}{2}\left[\Delta-\ln(m_b^2/\mu^2)+\tfrac{1}{2}\right]-\frac{m_{H^+}^2}{6m_b^2},$$

$$C_0=-\frac{1}{m_b^2},\quad C_{11}=\frac{1}{2m_b^2},\quad C_{12}=\frac{1}{4m_b^2},$$

$$C_{21}=-\frac{1}{3m_b^2},\quad C_{22}=-\frac{1}{9m_b^2},\quad C_{23}=-\frac{1}{6m_b^2},$$

$$C_{24}=\frac{1}{4}\left[\Delta-\ln(m_b^2/\mu^2)+\frac{1}{2}+\frac{3m_{H^+}^2+3m_W^2+2m_Z^2}{18m_b^2}\right],$$

$$\tilde{B}_1=-\tfrac{1}{2}[\Delta-\ln(m_b^2/\mu^2)+\tfrac{3}{2}]-\frac{m_{H^+}^2}{3m_b^2},$$

$$\tilde{C}_0=-\frac{1}{m_b^2}[\ln(-m_b^2/m_Z^2)+1],$$

$$\tilde{C}_{11}=\frac{1}{2m_b^2}[\ln(-m_b^2/m_Z^2)+\tfrac{3}{2}],$$

$$\tilde{C}_{12}=\frac{1}{2m_b^2},$$

$$\tilde{C}_{21}=-\frac{1}{3m_b^2}[\ln(-m_b^2/m_Z^3)+\tfrac{11}{6}],$$

$$\tilde{C}_{22}=-\frac{1}{6m_b^2},\quad \tilde{C}_{23}=-\frac{1}{3m_b^2},$$

$$\tilde{C}_{24}=\frac{1}{4}\left[\Delta-\ln(m_b^2/\mu^2)+\frac{3}{2}+\frac{m_Z^2}{3m_b^2}\ln(-m_b^2/m_Z^2)+\frac{6m_{H^+}^2+6m_W^2+5m_Z^2}{18m_b^2}\right].$$

### 4. $m_b=0$ ($R=\infty$)

One cannot simply take the $R\to\infty$ limit of the formulas of Appendix B 1 since some of the results would diverge. A separate calculation shows that these divergences are cut off by $m_Z$. The results below are valid for $m_b \ll m_Z, m_W, m_H \ll m_t$:

$$B_0=\Delta-\ln(m_t^2/\mu^2)+1+\frac{m_{H^+}^2}{2m_t^2},$$

$$B_1=-\tfrac{1}{2}[\Delta-\ln(m_t^2/\mu^2)+\tfrac{3}{2}]-\frac{m_{H^+}^2}{3m_t^2},$$

$$C_0=-\frac{1}{m_t^2}[\ln(-m_t^2/m_Z^2)+1],$$

$$C_{11}=\frac{1}{m_t^2}[\ln(-m_t^2/m_Z^2)+\tfrac{1}{2}],$$

$$C_{12}=\frac{1}{2m_t^2}[\ln(-m_t^2/m_Z^2)+\tfrac{1}{2}],$$

$$C_{21}=-\frac{1}{m_t^2}[\ln(-m_t^2/m_Z^2)+\tfrac{1}{6}],$$

$$C_{22}=-\frac{1}{3m_t^2}[\ln(-m_t^2/m_Z^2)+\tfrac{1}{3}],$$

$$C_{23}=-\frac{1}{2m_t^2}[\ln(-m_t^2/m_Z^2)+\tfrac{1}{6}],$$

$$C_{24}=\frac{1}{4}\left[\Delta-\ln(m_t^2/\mu^2)+\frac{3}{2}+\frac{m_Z^2}{3m_t^2}\ln(-m_t^2/m_Z^2)+\frac{6m_{H^+}^2+6m_W^2+5m_Z^2}{18m_t^2}\right],$$

$$\tilde{B}_1=-\tfrac{1}{2}[\Delta-\ln(m_t^2/\mu^2)+\tfrac{1}{2}]-\frac{m_{H^+}^2}{6m_t^2},$$

$$\tilde{C}_0=-\frac{1}{m_t^2},\quad \tilde{C}_{11}=\frac{3}{4m_t^2},\quad \tilde{C}_{12}=\frac{1}{2m_t^2},$$

$$\tilde{C}_{21}=-\frac{11}{18m_t^2},\quad \tilde{C}_{22}=-\frac{1}{3m_t^2},\quad \tilde{C}_{23}=-\frac{5}{12m_t^2},$$

$$\tilde{C}_{24}=\frac{1}{4}\left[\Delta-\ln(m_t^2/\mu^2)+\frac{1}{2}+\frac{3m_{H^+}^2+3m_W^2+2m_Z^2}{18m_t^2}\right].$$

Note the negative argument in $\ln(-m_t^2/m_Z^2)$ which appears in $C_0$ and $C_{ij}$ above. The imaginary part of the logarithm is a consequence of the existence of an on-shell decay $H^{\pm}\to W^{\pm}b\bar{b}$, followed by $t\bar{t}\to Z$.

It is important to note that the limits $m_Z\to 0$ and $m_b\to 0$ do not always commute. As an example, in Appendix B 1, we noted that for the leading term in the heavy-fermion-mass limit, $C_{21}=3C_{22}$. By explicit computation we find

$$C_{21}-3C_{22}\simeq\frac{-1}{m_t^2}\int_0^1 dx(3x^2-6x+2)\times\ln\left[\frac{m_b^2-x(1-x)m_Z^2}{m_t^2}\right].$$

If we set $m_Z=0$, the above integral vanishes. However, if we set $m_b=0$, we find $C_{21}-3C_{22}=1/(6m_t^2)$, in agreement with the results just obtained for the loop integrals in the $R\to\infty$ limit. Thus, in applying the above results, care is needed in deciding the correct order of the limits.


[1] For a comprehensive review of Higgs-boson physics, see J. F. Gunion, H. E. Haber, G. L. Kane, and S. Dawson, *The Higgs Hunter's Guide* (Addison-Wesley, Redwood City, CA, 1990).

[2] J. F. Gunion, H. E. Haber, S. Komamiya, H. Yamamoto, and A. Barbaro-Galtieri, in *Experiments, Detectors, and Experimental Areas for the Supercollider,* proceedings of the Workshop, Berkeley, California, 1987, edited by R. Donaldson and M. G. D. Gilchriese (World Scientific, Singapore, 1988), p. 110.

[3] J. F. Gunion, G. L. Kane, and J. Wudka, Nucl. Phys. **B299**, 231 (1988).

[4] J. A. Grifols and A. Mendez, Phys. Rev. D **22**, 1725 (1980); A. A. Iogansen, N. G. Ural'tsev, and V. A. Khoze, Yad. Fiz. **36**, 1230 (1982) [Sov. J. Nucl. Phys. **36**, 717 (1982)].

[5] J. F. Gunion, H. E. Haber, F. E. Paige, Wu-Ki Tung, and S. S. D. Willenbrock, Nucl. Phys. **B294**, 621 (1987).

[6] M. Capdequi Peyranere, H. E. Haber, and P. Irulegui (unpublished).

[7] S. Komamiya, Phys. Rev. D **38**, 2158 (1988).

[8] C. Ahn *et al.*, SLAC Report No. 329, 1988 (unpublished).

[9] A. Mendez and A. Pomarol, Nucl. Phys. **B349**, 369 (1991).

[10] In the standard $R_\xi$ gauge, the tadpole graphs do not sum to zero; nor is the sum of such graphs finite. The infinities cancel only when one adds a new graph obtained from Fig. 1(a) by replacing the internal $W$ propagator with that of the corresponding charged Goldstone boson. Remarkably, the cancellation of the tadpole graphs among themselves is restored by using the *nonlinear* $R_\xi$ gauge. Further details will be given in Ref. [6].

[11] S. Glashow and S. Weinberg, Phys. Rev. D **15**, 1958 (1977).

[12] M. Veltman, Nucl. Phys. **B123**, 89 (1977); M. Chanowitz, M. Furman, and I. Hinchliffe, Phys. Lett. **78B**, 285 (1978); Nucl. Phys. **B153**, 402 (1979); B. W. Lynn and R. G. Stuart, *ibid.* **B253**, 216 (1985); D. C. Kennedy and B. W. Lynn, *ibid.* **B322**, 1 (1989).

[13] The more general formulas can be found in P. Irulegui, Ph.D. dissertation, University of California, Santa Cruz, 1991.

[14] T. Rizzo, Mod. Phys. Lett. A **4**, 2757 (1989).

[15] H. E. Haber and G. L. Kane, Phys. Rep. **117**, 75 (1985).

[16] J. F. Gunion and H. E. Haber, Nucl. Phys. **B272**, 1 (1986).

[17] U. Amaldi, A. Bohm, L. S. Durkin, P. Langacker, A. K. Mann, and W. J. Marciano, Phys. Rev. D **36**, 1385 (1987).

[18] One of the authors of Ref. [3] has confirmed our results [J. Wudka (private communication)].

[19] G.'t Hooft and M. Veltman, Nucl. Phys. **B153**, 365 (1979); G. Passarino and M. Veltman, *ibid.* **B160**, 151 (1979).

[20] J. D. Bjorken and S. D. Drell, *Relativistic Quantum Mechanics* (McGraw-Hill, New York, 1964).

[21] R. G. Stuart, Comput. Phys. Commun. **48**, 367 (1987); **56**, 337 (1990).